Dynamical thresholds for compound-nucleus formation in symmetric heavy-ion reactions

K. Thomas R. Davies
Physics Division, Oak Ridge National Laboratory, Oak Ridge, Tennessee 37830

Arnold J. Sierk
Physics Division, Oak Ridge National Laboratory, Oak Ridge, Tennessee 37830
and Theoretical Division, Los Alamos National Laboratory, Los Alamos, New Mexico 87545

J. Rayford Nix
Theoretical Division, Los Alamos National Laboratory, Los Alamos, New Mexico 87545
(Received 13 January 1983)

We study the effect of the nuclear macroscopic energy, nuclear dissipation, and shape parametrization on dynamical thresholds for compound-nucleus formation in symmetric heavy-ion reactions. This is done by solving numerically classical equations of motion for head-on collisions to determine whether the dynamical trajectory in a multidimensional deformation space passes inside the fission saddle point and forms a compound nucleus, or whether it passes outside the fission saddle point and reseparates. Specifying the nuclear shape in terms of smoothly joined portions of three quadratic surfaces of revolution, we take into account three symmetric deformation coordinates. However, in some cases we reduce the number of coordinates to two by requiring the ends of the fusing system to be spherical in shape. The nuclear potential energy of deformation is determined in terms of a Coulomb energy and a nuclear macroscopic energy that is usually taken to be a double volume energy of a Yukawa-plus-exponential folding function, although a double volume integral of a single-Yukawa folding function and ordinary surface energy are also considered. The collective kinetic energy is calculated for incompressible, nearly irrotational flow by means of the Werner-Wheeler approximation. Four possibilities are studied for the transfer of collective kinetic energy into internal single-particle excitation energy: (1) zero dissipation, (2) ordinary two-body viscosity, (3) one-body wall-formula dissipation, and (4) one-body wall-and-window dissipation. For systems with Z^2/A larger than a threshold value $(Z^2/A)_{\rm thr}$ which depends somewhat upon dissipation, the center-of-mass bombarding energy must exceed the maximum in the one-dimensional interaction barrier by an amount ΔE in order to form a compound nucleus. For all four possibilities considered, we find that the dependence of ΔE on $Z^2/A-(Z^2/A)_{\rm thr}$ is more complicated than the lowest-order quadratic dependence found in some previous approximate solutions. For both types of one-body dissipation, our calculated values of ΔE are an order of magnitude larger than those for zero dissipation and ordinary two-body viscosity. We compare our results calculated for symmetric systems with experimental values for asymmetric systems by use of a tentative scaling involving $(Z^2/A)_{\rm mean}$, defined as the geometric mean of Z^2/A for the combined system and an effective value $(Z^2/A)_{\rm eff}$ for the projectile and target. When compared in this way, the experimental values of ΔE agree better with results calculated for two-body viscosity than with results calculated for either type of one-body dissipation.

[NUCLEAR REACTIONS $^{110}\mathrm{Pd}+{}^{110}\mathrm{Pd}\rightarrow{}^{220}\mathrm{U}$, symmetric nuclear systems leading to compound nuclei with $37.0\leq Z^2/A\leq 41.5$. Calculated dynamical thresholds for compound-nucleus formation. Macroscopic nuclear model, Yukawa-plus-exponential model, single-Yukawa model, liquid-drop model, nuclear inertia, nuclear dissipation, ordinary two-body viscosity, one-body dissipation, classical equations of motion, dynamical trajectory, compound-nucleus formation, heavy-ion fusion, fast fission, deep-inelastic reactions, time-dependent Hartree-Fock approximation.]

I. INTRODUCTION

A necessary condition for forming a compound nucleus in a heavy-ion reaction is that the dynamical trajectory of the fusing system pass inside the fission saddle point in a multidimensional deformation space. For nuclear systems lighter than a critical size and for relatively low angular momentum, the fission saddle point lies outside the point of hard contact in heavy-ion reactions, and this requirement is automatically satisfied once a one-dimensional interaction barrier is overcome. However, for heavier nuclear systems and/or for high angular momentum, the fission saddle point lies inside the contact point, and the center-of-mass bombarding energy must exceed the maximum in the one-dimensional interaction barrier by an amount ΔE in order to form a compound nucleus. This

was recognized[1-7] early, and more recently dynamical trajectories for fusing systems have been calculated by use of several approaches.[8-33]

In one approach,[8-18] the classical equations of motion were solved numerically for a system whose shape is specified in terms of smoothly joined portions of three quadratic surfaces of revolution. The nuclear potential energy of deformation was determined in terms of a Coulomb energy and a nuclear macroscopic energy usually given by a double volume integral of a Yukawa folding function but sometimes given by the surface energy of the liquid-drop model. The collective inertia tensor was calculated for nuclear flow that is a superposition of incompressible, nearly irrotational collective-shape motion and rigid-body rotation. Although some calculations were performed for asymmetric systems[12,15,18] and some included various types of dissipation,[12,15-18] most calculations with this approach were performed for symmetric systems with zero dissipation. These calculations illustrated that, even in the absence of dissipation, an additional bombarding energy ΔE relative to the maximum in the one-dimensional interaction barrier is required to form a compound nucleus for sufficiently heavy nuclear systems and/or sufficiently high angular momentum.

In another approach, pioneered by Swiatecki,[19-23] the classical equations of motion were solved approximately in closed form for a system whose shape is specified in terms of two spheres connected by a cylindrical neck in the original version[19] and by a conical neck in subsequent work.[20-23] The nuclear potential energy of deformation was parametrized by expanding the surface and Coulomb energies of the liquid-drop model to third order in the neck radius. For head-on collisions, all elements of the collective inertia tensor were neglected except the diagonal element corresponding to center-of-mass motion, which was taken equal to the reduced mass when the neck radius was less than a critical value and zero otherwise. Rotational kinetic energy was included approximately by mocking up the centrifugal force by an increase in the Coulomb repulsion. Nuclear dissipation was calculated by expanding the one-body wall-and-window formula to third order in the neck radius. The resulting approximate algebraic solution yielded a specific prediction for the additional bombarding energy ΔE relative to the maximum in the one-dimensional barrier required to form a compound nucleus. For nuclear systems with $(Z^2/A)_{\rm eff}$ larger than a threshold value $(Z^2/A)_{\rm thr}$, this additional energy ΔE, termed by Swiatecki the extra push, or under certain conditions the extra-extra push, was predicted to depend quadratically upon

$$(Z^2/A)_{\rm eff}-(Z^2/A)_{\rm thr}\ .$$

The quantity $(Z^2/A)_{\rm eff}$ is defined in terms of the individual projectile and target atomic numbers and mass numbers in such a way that for symmetric systems it reduces to Z^2/A for the combined system.

The solution of the above schematic model is characterized by five constants, some of whose values have been estimated both theoretically[20,24,25,26] and from comparisons with experimental data.[34-39] The original schematic model itself[20] yielded values for three of the constants that are significantly different from empirical values obtained from adjustments to experimental data, but improved models[24-26] yielded values in somewhat closer agreement with the empirical values. In these improved models, the nuclear shape was specified in terms of two spheres connected smoothly by a hyperboloidal neck, the collective potential and kinetic energies and one-body wall-and-window dissipation were calculated more accurately, and the equations of motion were integrated numerically.

In still another approach,[27-33] the time-dependent Hartree-Fock (TDHF) equations of motion were integrated numerically for a two- or three-dimensional grid. For moderately heavy systems, the onset of fusion is at an energy considerably above the maximum in the interaction barrier, and this phenomenon is at least qualitatively related to the energy thresholds found in the macroscopic studies.[8-26] Whereas in macroscopic calculations one of the main uncertainties affecting the fusion behavior is the choice of an appropriate dissipation model, in the TDHF approximation the dissipation is caused only by one-body collisions with the mean-field potential. However, in the TDHF calculations there can be very large threshold-energy discrepancies arising from the choice of the two-body interaction used. For example, it has been demonstrated[32] in studies of ^{86}Kr + ^{139}La that the laboratory-energy fusion threshold for the Skyrme III potential is more than 150 MeV lower than that for the Skyrme II potential. Also, the TDHF results[32] for the Skyrme II potential exhibit a very pronounced fusion behavior at an energy just above the maximum in the interaction barrier, which is reminiscent of the adiabatic slither or cold fusion predicted in Ref. 22. In addition to the above type of energy threshold, a completely different type occurs in the TDHF approximation for all nuclear systems at a relatively high energy, where it is found that fusion abruptly disappears for head-on collisions.[30,32] For energies above this threshold, there exists a low-angular-momentum cutoff below which there is no fusion. This behavior is intimately connected with the transparency inherent in the mean-field approximation and has not been verified experimentally.

The various theoretical approaches discussed above all predict that for sufficiently heavy nuclear systems and/or high angular momentum, the center-of-mass bombarding energy must exceed the maximum in the one-dimensional interaction barrier by an amount ΔE in order to form a compound nucleus. The necessity for such an additional energy has been suggested experimentally in several recent studies,[21-23,34-45] although an alternate interpretation in terms of large surface friction has been proposed.[46] (The opposite conclusion obtained in an earlier study[47] was based on comparisons with a schematic model[20] whose estimated constants are now known to be unreliable.) Although the comparisons with experimental data have sometimes been interpreted as evidence for one-body wall-and-window dissipation, it must be borne in mind that the additional energy arises from the need to overcome both repulsive Coulomb and/or centrifugal forces on one hand and dissipative forces on the other hand. In the comparisons made to date, no attempt has been made to distinguish between conservative and dissipative forces.

Although the effect of various types of dissipation on the dynamical motion has been calculated for a few special cases,[12,15-18] there is a strong need for a systematic

study of this question. It is our major purpose here to calculate within a single unified model the dependence of the additional energy ΔE upon Z^2/A for various types of dissipation, in an effort to ultimately determine the magnitude and mechanism of nuclear dissipation from comparisons with experimental data. Since both our predictions and those of other groups depend somewhat upon the details of the model, we also study the effect of the nuclear macroscopic energy and the shape parametrization on the dynamical thresholds. Our dynamical model is described in Sec. II, and our calculated results are presented in Sec. III. In Sec. IV we compare our results calculated for symmetric systems with experimental data for asymmetric systems by use of a tentative scaling, and in Sec. V we summarize and conclude our paper. Appendix A discusses the method that we use to integrate the equations of motion during the approach and contact stages until an appreciable neck has developed, and Appendix B discusses the functional dependence of ΔE on $Z^2/A-(Z^2/A)_{\rm thr}$.

II. DYNAMICAL MODEL

Detailed discussions exist elsewhere[13,14,48–50] for both the dynamical model and numerical methods that we use in our present studies. Therefore, we discuss only briefly those aspects relevant to our present calculations. The main results of this paper are obtained from dynamical calculations for head-on collisions of two symmetric heavy ions, together with static calculations of the fission saddle points for the combined systems.

The nuclear shape is described by means of the three-quadratic-surface parametrization,[48,49] in which an axially symmetric shape consists of smoothly joined portions of three quadratic surfaces of revolution. For this paper we also assume reflection symmetry about a plane through the geometrical center of the middle body and perpendicular to the symmetry axis, which restricts our studies to mass-symmetric collisions. In this parametrization symmetric shapes are described by three independent collective coordinates, but it is convenient to project out of this three-dimensional space two moments of the distribution that have special physical significance. These are defined by[13,49–51]

$$r=2\langle z\rangle \tag{1}$$

and

$$\sigma=2\langle(z-\langle z\rangle)^2\rangle^{1/2}\ , \tag{2}$$

where z is measured along the symmetry axis and the angular brackets denote an average over the half volume to the right of the midplane of the reflection-symmetric shape. The moment r gives the distance between the mass centers of the two colliding ions, while σ measures the fragment elongation or the necking in the combined system.

For both the static and dynamical calculations, we determine the potential energy of deformation from the sum of the Coulomb electrostatic energy and a nuclear macroscopic energy, namely,

$$V(q_1,q_2,\ldots,q_N)\equiv V(q)=V_{\rm Coul}(q)+V_{\rm nucl}(q)\ , \tag{3}$$

where q_i denotes one of the N collective coordinates used to describe the shape. Most of our results are obtained with the Yukawa-plus-exponential (YPE) nuclear macroscopic energy,[52,53] with values of the constants determined in Refs. 54 and 55. This energy takes into account the nonzero range of the nuclear force, saturation at the contact point for two semi-infinite slabs of nuclear matter, and the curvature of the nuclear surfaces for finite nuclei. Also, the constants that enter this energy have values that are determined systematically from diverse physical considerations, namely the nuclear-radius constant r_0 from elastic-electron scattering, the surface-energy constant a_s and surface-asymmetry constant κ_s from fission-barrier heights, and the range a from heavy-ion elastic scattering. The resulting heavy-ion interaction potential correctly describes experimental fusion barriers for light nuclei automatically, even though such data were not used in the determination of the constants.[52,53] In addition to using the Yukawa-plus-exponential nuclear macroscopic energy, for a few cases we show the effects of using either the single-Yukawa (SY) energy[51,56] or the surface energy of the liquid-drop model (LDM).[57]

For the dynamical calculations for head-on collisions, the collective kinetic energy is given by

$$T=\tfrac{1}{2}\sum_{i,j=1}^{N}M_{ij}(q)\dot{q}_i\dot{q}_j=\tfrac{1}{2}\sum_{i,j=1}^{N}(M^{-1})_{ij}p_ip_j\ , \tag{4}$$

where p_i is the momentum conjugate to q_i and $M_{ij}(q)$ is a shape-dependent inertia tensor obtained by use of the Werner-Wheeler approximation to incompressible, irrotational flow.[48,49]

We consider the case of zero dissipation, as well as three different types of dissipative forces: ordinary two-body viscosity with a viscosity coefficient $\mu=0.02$TP,[49,50,58] one-body wall-formula dissipation,[59,60] and one-body wall-and-window dissipation.[50,59,60] The viscosity coefficient $\mu=0.02$TP is chosen because this value[58] optimally reproduces average fission-fragment kinetic energies for the fission of nuclei at high excitation energies throughout the Periodic Table, when the most recent constants of the Yukawa-plus-exponential potential[54,55] are used. The two types of one-body dissipation differ from each other in the following way: In the wall formula all velocities normal to the nuclear surface are measured relative to the stationary center of mass of the combined system and no window term is included, whereas in the wall-and-window formula surface normal velocities for a given half of the system are measured relative to the moving center of mass of that half, and an additional term is included to describe dissipation arising from the flux of particles through the window separating the two halves.[59,60] The dissipative forces are included by means of the Rayleigh dissipation function[49,61]

$$F=\tfrac{1}{2}\sum_{i,j=1}^{N}\eta_{ij}(q)\dot{q}_i\dot{q}_j\ , \tag{5}$$

where η_{ij} is the shape-dependent viscosity tensor appropriate to a particular type of dissipation.

The dynamical evolution of the nuclear shape is obtained by solving the generalized Hamilton equations of motion[49]

$$\dot{q}_i = \sum_{j=1}^{N} (M^{-1})_{ij} p_j, \quad i = 1,2,\ldots N \tag{6}$$

and

$$\dot{p}_i = -\frac{\partial V}{\partial q_i} - \tfrac{1}{2} \sum_{j,k=1}^{N} \frac{\partial (M^{-1})_{jk}}{\partial q_i} p_j p_k - \sum_{j,k=1}^{N} \eta_{ij} (M^{-1})_{jk} p_k, \quad i = 1,2,\ldots N . \tag{7}$$

Because of numerical difficulties associated with the three-quadratic-surface parametrization for shapes near two touching spheres, we describe the approach and contact stages by use of a simpler method discussed in Appendix A. After the radius of the neck between the two ions attains a certain transition value r_n, we then switch to the three-quadratic-surface parametrization. The transition radius r_n is taken to be 3.0 fm except for wall-and-window dissipation, where we are forced to use a value of 3.5 fm because of numerical difficulties.

III. CALCULATED RESULTS

In our studies of the dynamics of heavy-ion reactions, we are especially concerned with whether a particular collision leads to compound-nucleus formation. For this purpose, we plot in r-σ deformation space both the dynamical trajectory for a particular reaction and the location of the saddle point for the combined system. The criterion[13] adopted for compound-nucleus formation is that the trajectory in r-σ space pass inside (to the left of) the saddle point. When the trajectory passes outside (to the right of) the saddle point, the system reseparates in a fast-fission[62] or deep-inelastic reaction.

We also obtain the threshold energy for compound-nucleus formation. This minimum energy required to produce a compound nucleus is determined by finding the dynamical trajectory that just passes through the saddle point. Since our calculations are for mass-symmetric reactions, there is no difference here between the true saddle point and the conditional saddle point for fixed mass asymmetry.[19–25] Thus, the fusion that we obtain is exclusively compound-nucleus formation, with no contribution from mass-equilibrated fast fission.[62]

We now present two different types of calculated results. First, for the particular reaction $^{110}\mathrm{Pd} + {}^{110}\mathrm{Pd} \rightarrow {}^{220}\mathrm{U}$, we show how compound-nucleus formation depends upon various details of the model used, especially the choice of nuclear macroscopic energy, the type of dissipation, and the shape parametrization. Second, for each type of dissipation considered, we determine energy thresholds for different nuclear reactions characterized by the value of Z^2/A for the combined system. For this second type of result, we are especially interested in the dependence upon Z^2/A of the additional energy ΔE relative to the maximum in the one-dimensional interaction barrier required for compound-nucleus formation.

A. The reaction $^{110}\mathrm{Pd} + {}^{110}\mathrm{Pd} \rightarrow {}^{220}\mathrm{U}$

To aid in interpreting the dynamical trajectories that will follow, we show in Fig. 1 a contour map in r-σ space of the nuclear potential energy of deformation for the reaction $^{110}\mathrm{Pd} + {}^{110}\mathrm{Pd} \rightarrow {}^{220}\mathrm{U}$, calculated in terms of a Coulomb energy and a nuclear macroscopic energy given

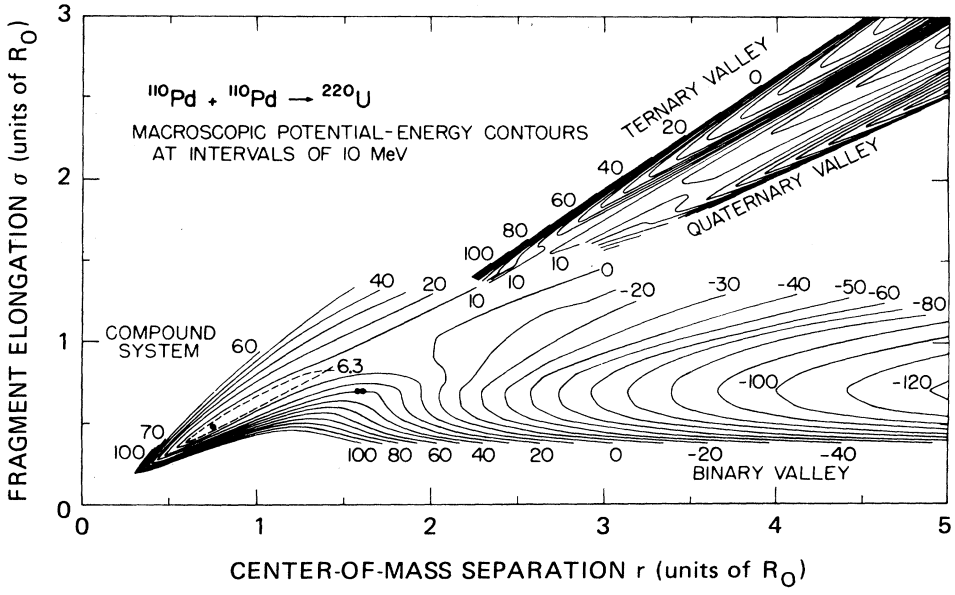

FIG. 1. Potential-energy contours, in units of MeV, for the reaction $^{110}\mathrm{Pd} + {}^{110}\mathrm{Pd} \rightarrow {}^{220}\mathrm{U}$, calculated with a single-Yukawa macroscopic model (Ref. 51). The moment r is the distance between the centers of mass of the two halves of the system, and the moment σ is the sum of the root-mean-square extensions along the symmetry axis of the mass of each half about its center of mass, both measured in units of the radius R_0 of the combined system. The location of the sphere is given by the solid point, and the location of two touching spheres is given by two adjacent solid points.

TABLE I. Calculated additional energy ΔE relative to the maximum in the one-dimensional interaction barrier required to form a compound nucleus in a head-on collision for $^{110}Pd+^{110}Pd \rightarrow ^{220}U$. The transition neck radius r_n is 3.0 fm unless indicated otherwise.

Nuclear macroscopic energy	Dissipation	ΔE (MeV) Full three-quadratic-surface parametrization	Spherical ends
Liquid-drop model	No dissipation	0	
Single Yukawa	No dissipation	0	
Single Yukawa	No dissipation, $r_n=1.0$ fm	3.80±0.05	
Yukawa plus exponential	No dissipation	1.5 ±0.2	4.5±0.1
Yukawa plus exponential	Two-body viscosity, $\mu=0.02$TP	5±0.5	0.5±0.5
Yukawa plus exponential	Wall formula	90±2	60±2
Yukawa plus exponential	Wall and window		36±0.5
Yukawa plus exponential	Wall and window, $r_n=3.5$ fm	39±0.5	32±0.5

by a double volume integral of a single-Yukawa folding function.[51,56] In this reaction, the two separated spherical ^{110}Pd nuclei move up the binary valley near the bottom of the figure from right to left, and come into solid contact at the point indicated by the two adjacent solid circles. This point is slightly inside the maximum in the one-dimensional interaction barrier calculated as a function of r alone, but is on the side of a steep hill with respect to fragment elongation (increasing σ). In order for a compound nucleus to be formed, the dynamical trajectory must pass inside the fission saddle point, located at the intersection of the dashed 6.3-MeV contours, and become trapped in the potential-energy hollow surrounding the sphere, whose location is indicated by the solid circle.

For this reaction typical results are shown in Figs. 2–8, and the threshold energies are summarized in Table I. In the figures and table, the additional energy ΔE is defined as the difference between the bombarding energy in the center-of-mass system and the maximum in the one-dimensional interaction barrier. However, in the figures ΔE denotes an arbitrary energy over the barrier top, whereas in the table ΔE denotes the minimum energy required for compound-nucleus formation, determined by finding the trajectory which passes through the saddle point.

In the figures the bold, horizontal arrow from the right-hand border to the solid circle denoting tangent spheres represents the last part of the trajectory from infinite separation to just touching. During this stage and continuing along the short, bold arrow from the solid circle denoting the tangent spheres to the open circle, the dynamical evolution is described by use of the simple model discussed in Appendix A. For all cases except wall-and-window dissipation, the three-quadratic-surface parametrization is used starting at the open circle, where the neck radius r_n is 3.0 fm. At this point the values of the moments are $r/R_0=1.458$ and $\sigma/R_0=0.709$ for this system. Because of numerical difficulties, for wall-and-window dissipation the simple model discussed in Appendix A is used until the neck radius is 3.5 fm, where the corresponding values of the moments are $r/R_0=1.408$ and $\sigma/R_0=0.707$.

For the case of zero dissipation and additional energy $\Delta E=20$ MeV, we display in Fig. 2 the calculated saddle-point configurations and dynamical trajectories for three different nuclear macroscopic energies. These energies correspond to the single-Yukawa model,[51,56] which has been used in previous dynamical calculations[13,14] and whose potential-energy contours are shown in Fig. 1; the liquid-drop model,[57] which has also been used in previous dynamical calculations[8,14]; and the Yukawa-plus-exponential model[52,53] with constants determined in Refs. 54 and 55, which is used for the remaining calculations presented in this paper. We see in Fig. 2 that the dynamical trajectories for all three nuclear macroscopic energies lie fairly close together. However, as seen in Table I, there are some dynamical differences since the additional threshold energy ΔE is 1.5, 0, and 0 MeV for the YPE, LDM, and SY nuclear macroscopic energies, respectively.

Comparing the two finite-range nuclear macroscopic energies, we see in Fig. 2 that the SY saddle-point shape is

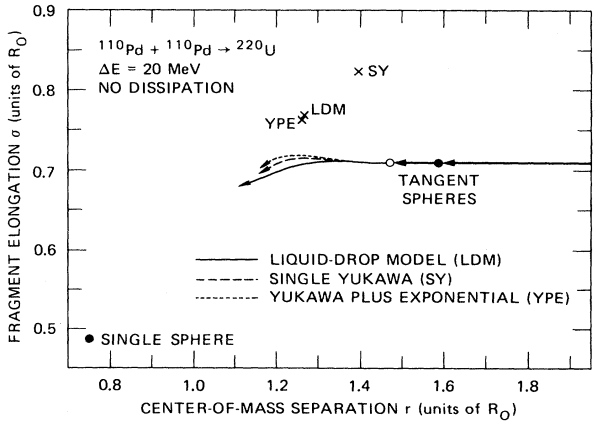

FIG. 2. Effect of the nuclear macroscopic energy on saddle-point configurations and dynamical trajectories in the r-σ plane for the reaction $^{110}Pd+^{110}Pd \rightarrow ^{220}U$ at $\Delta E=20$ MeV, calculated for zero dissipation. The interval ΔE is defined as the difference between the bombarding energy in the center-of-mass system and the maximum in the one-dimensional interaction barrier. Solid circles indicate the single-sphere and tangent-spheres configurations, and the open circle indicates where the three-quadratic-surface numerical integration begins. For each type of nuclear macroscopic energy the saddle-point configuration for the combined system is indicated by a cross (×).

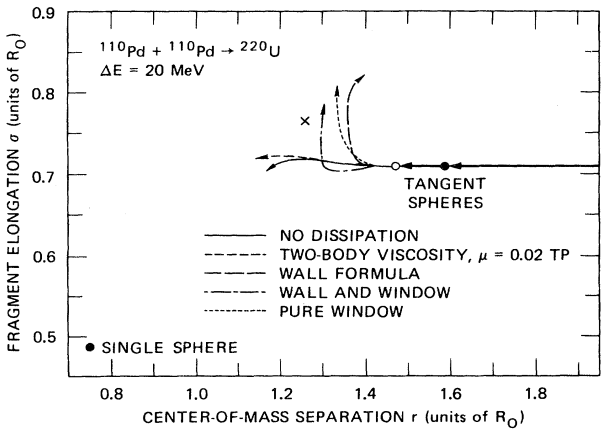

FIG. 3. Effect of dissipation on dynamical trajectories in the r-σ plane for the reaction $^{110}Pd+{}^{110}Pd \rightarrow {}^{220}U$ at $\Delta E=20$ MeV in the full three-quadratic-surface parametrization.

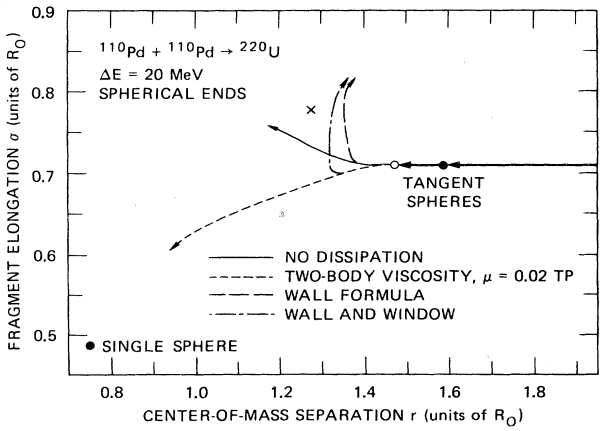

FIG. 4. Effect of dissipation on dynamical trajectories in the r-σ plane for the reaction $^{110}Pd+{}^{110}Pd \rightarrow {}^{220}U$ at $\Delta E=20$ MeV when the end bodies are constrained to be spherical. (In this figure the transition neck radius r_n is 3.0 fm also for wall-and-window dissipation.)

considerably more elongated than the YPE saddle-point shape. Because of this, the SY nuclear macroscopic energy permits fusion at a lower bombarding energy than does the YPE nuclear macroscopic energy. Although the YPE and LDM saddle points lie very close together, the corresponding energy thresholds differ slightly. Table I also lists the result from Ref. 13 for the SY nuclear macroscopic energy and zero dissipation, but calculated using the smaller transition neck radius $r_n=1.0$ fm. Comparing the two SY cases, we see that increasing r_n by 2.0 fm decreases the nondissipative threshold energy by at least 3.8 MeV.

For the remaining calculations in this paper we use exclusively the YPE nuclear macroscopic energy. In Fig. 3 we compare dynamical trajectories for five different types of dissipation. In addition to the four types previously mentioned, we include an example of pure window dissipation, obtained by omitting the wall contribution in wall-and-window dissipation. We note that the dynamical paths for no dissipation and two-body viscosity prefer changes in separation r rather than neck formation σ. The curves for no dissipation and two-body viscosity are not very different since the viscosity coefficient $\mu=0.02$TP is relatively small. On the other hand, the one-body-dissipation models all generate trajectories in which σ changes much more rapidly than r. Such behavior has previously been observed in calculations of fission.[49,50]

By comparing Figs. 3 and 4, we see the effect of constraining the end bodies to be spherical. In this widely used approximation,[19–26] both the first and third surfaces in the three-quadratic-surface parametrization are forced to be spheres. The most dramatic change is for two-body viscosity, whose trajectory in Fig. 4 leads to much more compressed shapes than the corresponding trajectory in Fig. 3. For the energy thresholds, we observe from Table I that there can be substantial discrepancies arising from the approximation of using spherical end bodies. In particular, for the wall formula the additional threshold energy ΔE is about 30 MeV larger when the spherical constraint is not imposed. For wall-and-window dissipation with spherical end bodies it is possible to use a transition neck radius of $r_n=3.0$ fm without encountering numerical difficulties. As seen in Table I, increasing r_n from 3.0 to 3.5 fm in this case decreases ΔE by about 4 MeV.

In Figs. 5–8 we show, for each type of dissipation considered, the behavior of the dynamical trajectories as the center-of-mass bombarding energy is changed. For each case except the nondissipative one we display curves for $\Delta E=0.5$ and 20 MeV, as well as the threshold value, for which the trajectory passes through the saddle point. For the nonviscous case, the lowest energy trajectory is for 0 MeV. In wall-formula dissipation (Fig. 7) we also plot the very high-energy trajectory corresponding to $\Delta E=150$ MeV. These figures all illustrate that with increasing bombarding energy, the two ions interpenetrate more, giving rise to more compressed shapes. However, for both types of one-body dissipation, the system strongly resists compound-nucleus formation. This feature is especially pronounced for the wall formula because the velocities normal to the nuclear surface are measured relative to the stationary center of mass of the combined system and are larger than those measured relative to the moving centers of mass of each half of the system.

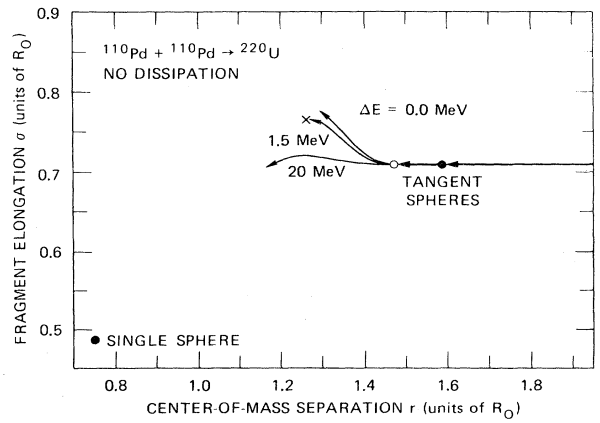

FIG. 5. Effect of bombarding energy on dynamical trajectories in the r-σ plane for the reaction $^{110}Pd+{}^{110}Pd \rightarrow {}^{220}U$, calculated for zero dissipation.

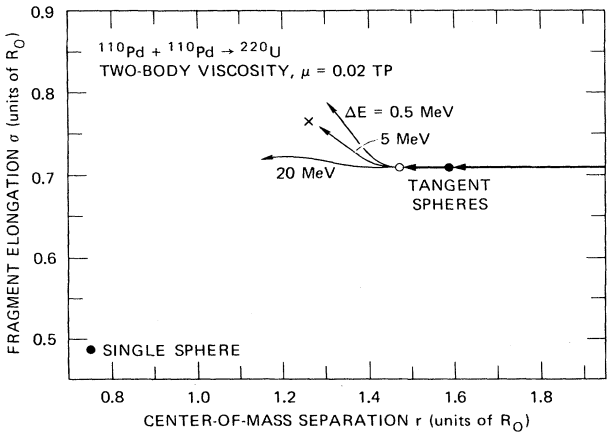

FIG. 6. Effect of bombarding energy on dynamical trajectories in the r-σ plane for the reaction ^{110}Pd+^{110}Pd→^{220}U, calculated for two-body viscosity with coefficient $\mu=0.02$TP.

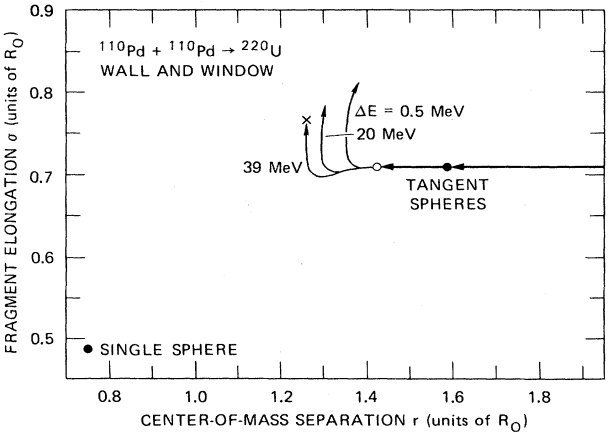

FIG. 8. Effect of bombarding energy on dynamical trajectories in the r-σ plane for the reaction ^{110}Pd+^{110}Pd→^{220}U, calculated for wall-and-window dissipation. (In this figure the open circle denotes a transition neck radius of 3.5 fm.)

B. Dynamical thresholds for different systems

We now study the fusion behavior for different heavy-ion reactions, which we designate by the value of Z^2/A for the combined system. The total atomic number is $Z=Z_1+Z_2$ and the total mass number is $A=A_1+A_2$, with the subscripts 1 and 2 referring to the projectile and target, respectively. Because we assume reflection symmetry, $Z_1=Z_2$ and $A_1=A_2$, so that Z^2/A is identically equal to both the effective value (Refs. 19–26, 34–41, 43, 44, and 47)

$$(Z^2/A)_{\text{eff}}=4Z_1Z_2/[A_1^{1/3}A_2^{1/3}(A_1^{1/3}+A_2^{1/3})] \tag{8}$$

and the geometric mean (Refs. 23, 24, 36–39, and 41)

$$(Z^2/A)_{\text{mean}}=[(Z^2/A)(Z^2/A)_{\text{eff}}]^{1/2} . \tag{9}$$

Since

$$Z_1^2/A_1=Z_2^2/A_2=\tfrac{1}{2}Z^2/A , \tag{10}$$

we can easily determine the individual atomic and mass numbers from the requirement that the projectile and target each lie along the valley of β stability according to Green's approximation[63]

$$A_i-2Z_i=0.4A_i^2/(200+A_i), \quad i=1,2 . \tag{11}$$

This is in contrast to some earlier dynamical threshold studies,[19–22] where the combined system was taken to lie along Green's approximation to the valley of β stability. As shown by Feldmeier,[25] this leads to significant differences in the calculated results.

In Figs. 9 and 10 typical r-σ graphs are displayed for two types of dissipation, with $\Delta E=0.5$ MeV. In each figure we plot the saddle-point configurations and dynamical trajectories for three different values of Z^2/A, including that value for which the trajectory passes through the saddle point. These two figures clearly show that, as we change Z^2/A, the saddle-point configurations are dis-

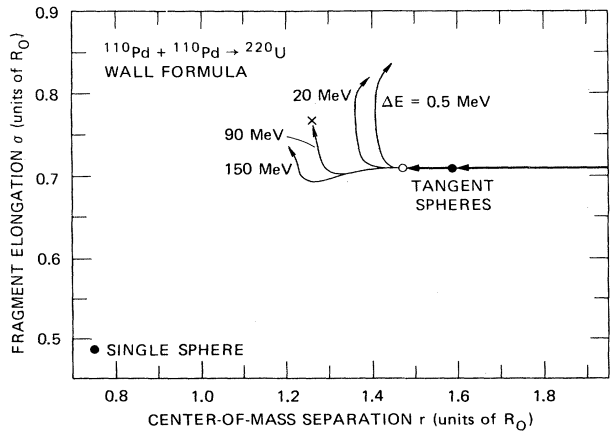

FIG. 7. Effect of bombarding energy on dynamical trajectories in the r-σ plane for the reaction ^{110}Pd+^{110}Pd→^{220}U, calculated for wall-formula dissipation.

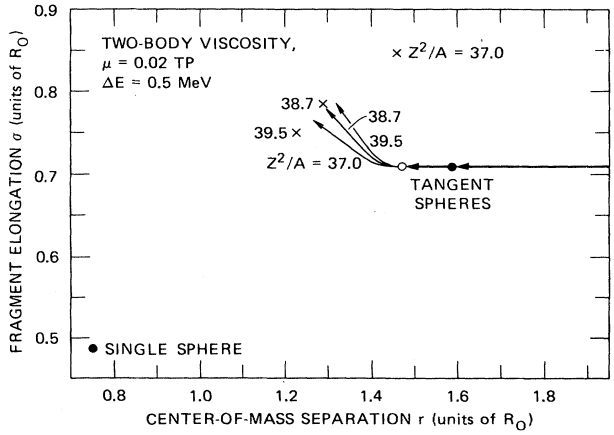

FIG. 9. Effect of the nuclear system on saddle-point configurations and dynamical trajectories in the r-σ plane for $\Delta E=0.5$ MeV, calculated for two-body viscosity with coefficient $\mu=0.02$TP. Each saddle point and trajectory is labeled by the value of Z^2/A for the combined system, with the symmetric target and projectile chosen to lie along Green's approximation to the valley of β stability (Ref. 63).

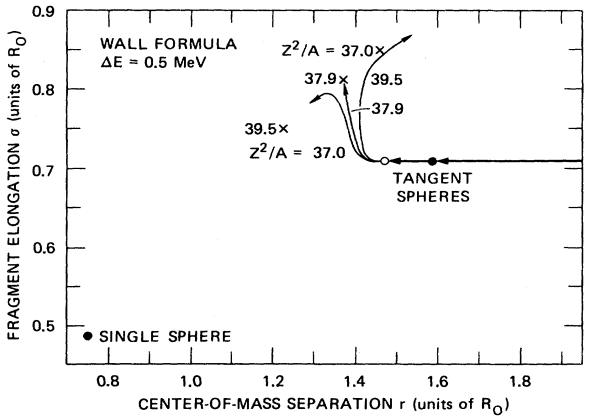

FIG. 10. Effect of the nuclear system on saddle-point configurations and dynamical trajectories in the r-σ plane for $\Delta E=0.5$ MeV, calculated for wall-formula dissipation.

placed much more than the trajectories. As the charge on the system increases, the saddle point moves to a more compact configuration, while the trajectory is deflected in the opposite direction. In passing, we remark that the effect of angular momentum is qualitatively similar to that of charge regarding the behavior of saddle points and trajectories.[13,20–23]

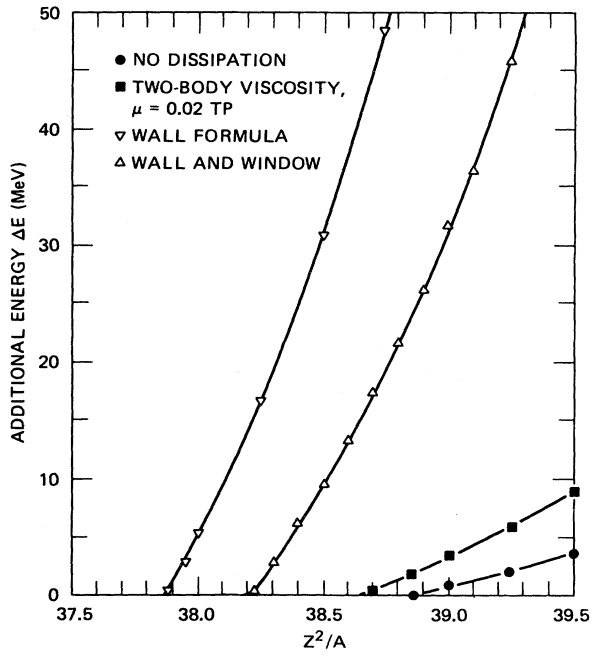

FIG. 11. Effect of dissipation on the additional center-of-mass bombarding energy ΔE relative to the maximum in the one-dimensional interaction barrier required to form a compound nucleus in a head-on collision. The smooth curves are drawn by hand through the calculated points taken from Table II. The value of Z^2/A refers to the combined system, with the symmetric target and projectile chosen to lie along Green's approximation to the valley of β stability (Ref. 63).

Additional calculations have been carried out for a wide range of reactions using all four types of dissipation. The final threshold values are summarized in Table II and plotted in Fig. 11. For $\Delta E=0$ (no dissipation) or 0.5 MeV (nonzero dissipation), we use graphs like Figs. 9 and 10 to find the value of Z^2/A for which the trajectory passes through the corresponding saddle point. This value of Z^2/A is determined to within ± 0.01. For all other cases, Z^2/A is fixed and a search is made for ΔE, which is usually determined to within ± 0.1 MeV. However, for a few cases, the trajectories terminate before reaching the saddle point because of a breakdown in the three-quadratic-surface parametrization, and the threshold energy must be determined by subjective extrapolation, which gives rise to an estimated error in $|\Delta E|$ that is larger than 0.1 MeV. We also list in Table II the threshold value $(Z^2/A)_{\rm thr}$ corresponding to $\Delta E=0$, which for nonzero dissipation is determined by graphical extrapolation in Fig. 11.

When comparing the results for the different types of dissipation in Table II and Fig. 11, we must remember that for the transition neck radius we have used $r_n=3.5$ fm for wall-and-window dissipation and $r_n=3.0$ fm for the other cases. From our study of ^{110}Pd + ^{110}Pd in the previous subsection, we saw that whereas the dynamical behavior is not drastically sensitive to the choice of r_n, a larger value of r_n reduces the threshold energy somewhat.

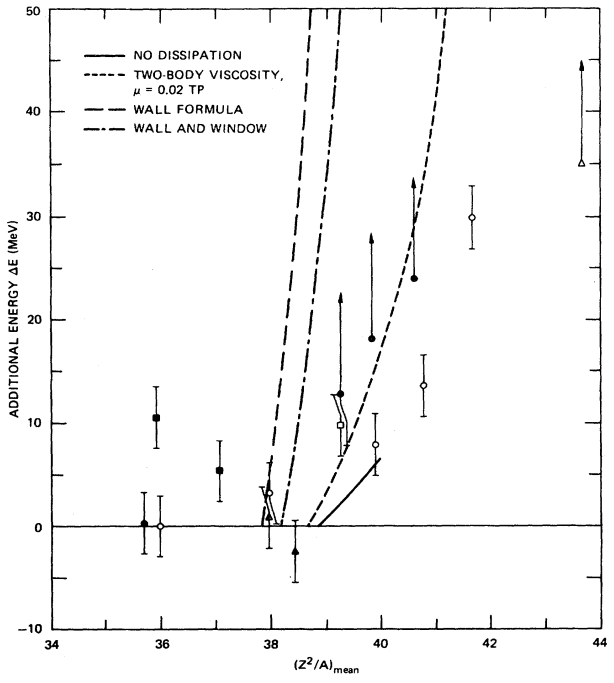

FIG. 12. Comparison of additional energy ΔE required for compound-nucleus formation calculated for symmetric systems with experimental values for asymmetric systems characterized by $(Z^2/A)_{\rm mean}$, defined by Eq. (9). Values extracted from evaporation-residue measurements are represented by solid symbols (●, Ref. 42; ■, Ref. 47; and ▲, Ref. 41), whereas values extracted from measurements of nearly symmetric fissionlike fragments are represented by open symbols (○, Ref. 23; □, Ref. 45; and △, Ref. 43).

TABLE II. Additional center-of-mass bombarding energy ΔE relative to the maximum in the one-dimensional interaction barrier required to form a compound nucleus in a head-on collision, calculated with the Yukawa-plus-exponential nuclear macroscopic energy. The transition neck radius r_n is 3.0 fm except for wall-and-window dissipation, where it is 3.5 fm. The value of Z^2/A in each case refers to the combined system, with the symmetric target and the projectile chosen to lie along Green's approximation to the valley of β stability (Ref. 63).

Dissipation	Z^2/A	ΔE (MeV)
No dissipation	38.87±0.01[b]	0
	39.0	0.8±0.1
	39.25	2.0±0.2
	39.5	3.5±0.5
	40.0	6.5±0.5
Two-body viscosity $\mu=0.02TP$	38.65[a]	0
	38.70±0.01[b]	0.5
	38.85	1.9±0.1
	39.0	3.5±0.1
	39.25	6.0±0.1
	39.5	9.0±0.1
	40.0	16.9±0.1
	40.5	26.0±0.5
	41.0	40.0±0.2
	41.5	59 ±1
Wall formula	37.87[a]	0
	37.88±0.01[b]	0.5
	37.9	1.5±0.1
	37.95	2.8±0.1
	38.0	5.4±0.1
	38.25	16.8±0.1
	38.5	31.0±0.1
	38.75	48.5±0.1
	39.0	67.5±0.1
	39.5	130.2±0.1
Wall and window	38.22[a]	0
	38.23±0.01[b]	0.5
	38.3	2.8±0.1
	38.4	6.2±0.1
	38.5	9.5±0.1
	38.6	13.4±0.1
	38.7	17.5±0.1
	38.8	21.6±0.1
	38.9	26.2±0.1
	39.0	31.8±0.1
	39.1	36.5±0.1
	39.25	45.9±0.1
	39.5	63.0±0.1

[a]Obtained by graphical extrapolation in Fig. 11.
[b]Search is made for Z^2/A at fixed ΔE.

In addition, as discussed in Appendix B, use of a nonzero value of r_n introduces a linear component in the dependence of ΔE on $Z^2/A-(Z^2/A)_{\rm thr}$. To lowest order ΔE depends quadratically[20–23] on $Z^2/A-(Z^2/A)_{\rm thr}$ when the initial conditions correspond to starting with spheres at the top of the one-dimensional interaction barrier moving radially inward with kinetic energy ΔE. However, this lowest-order quadratic dependence is destroyed when dynamical effects that occur during the approach and contact stages are taken into account. Also, quantal subbarrier tunneling destroys the quadratic dependence. Therefore, little physical significance should be attached to the lowest-order functional dependence of ΔE on $Z^2/A-(Z^2/A)_{\rm thr}$ and consequently to the precise value of $(Z^2/A)_{\rm thr}$. Instead, attention should be focused on the rate of increase of ΔE with increasing Z^2/A somewhat above the threshold.

As seen in Fig. 11, for both types of one-body dissipation our calculated values of ΔE are in general an order of magnitude larger than those for zero dissipation and ordinary two-body viscosity. The values of ΔE for wall-formula dissipation are larger than those for wall-and-

window dissipation primarily because the surface normal velocities measured relative to the stationary center of mass of the entire system in the former case are larger than the normal velocities measured relative to the moving centers of mass of each half of the system in the latter case.

IV. COMPARISON WITH EXPERIMENTAL DATA

In order to compare the additional energy ΔE required for compound-nucleus formation that we have calculated for symmetric systems with experimental values, it is necessary to scale the asymmetric nuclear systems that are studied experimentally into symmetric ones. Although the effective value $(Z^2/A)_{\text{eff}}$ defined by Eq. (8) has been frequently used for this purpose (Refs. 19–26, 34–41, 43, 44, and 47) the dynamical calculations performed for asymmetric systems by Feldmeier[25] and more recently by Błocki and Swiatecki[24] indicate that this simple scaling based on the projectile and target at contact does not hold. Because the dynamical trajectory of a fusing system moves from the contact region, where $(Z^2/A)_{\text{eff}}$ is appropriate, to the saddle-point region, where Z^2/A for the combined system is appropriate, scaling in terms of the geometric mean $(Z^2/A)_{\text{mean}}$ defined[23,24,36–39,41] by Eq. (9) should be more accurate. This expectation can be verified by replotting the results presented in Fig. 4 of Ref. 25 versus $(Z^2/A)_{\text{mean}}$ instead of $(Z^2/A)_{\text{eff}}$, which largely reconciles Feldmeier's calculations for asymmetric systems with those for symmetric systems presented in Table 1 of Ref. 25. The more recent calculations for asymmetric systems by Błocki and Swiatecki[24] also support the choice of $(Z^2/A)_{\text{mean}}$ for a scaling variable.

Although remaining uncertainties associated with scaling preclude a definitive comparison at this stage, we nevertheless compare in Fig. 12 calculated and experimental[23,41–43,45,47] values of the additional center-of-mass bombarding energy ΔE required for compound-nucleus formation. The experimental values indicated by solid symbols are extracted from measurements of evaporation residues,[41,42,47] which require the formation of true compound nuclei. The experimental values indicated by open symbols are extracted from measurements of nearly symmetric fissionlike fragments,[23,35,43,45] where fast-fission processes involving significant mass transfer but not true-compound-nucleus formation also contribute. For both the solid and open symbols, the experimental values of the additional energy ΔE are determined by subtracting from the experimental barrier heights extrapolated values that correctly reproduce the smooth trends for somewhat lighter nuclei. For consistency with recent practice,[21–23,41] these extrapolated values are taken to be 96% of the barrier heights calculated[41] with the proximity potential[64] for all cases except the open triangle, where the procedure of Ref. 43 is followed. Had we used instead the full barrier heights calculated with the Yukawa-plus-exponential potential, the major effect would have been to systematically shift the experimental points in Fig. 12 downward by about 10 MeV, although the amount of the shift would have been somewhat larger for nearly symmetric systems than for asymmetric systems. The former procedure is used here because it better reproduces the barrier heights of those nuclei with $(Z^2/A)_{\text{mean}}$ slightly below the critical value where an additional energy ΔE is predicted to be required. However, had the latter procedure been used, our final conclusion concerning the magnitude and mechanism of nuclear dissipation would be even stronger. For the open triangle[43] corresponding to radiochemical measurements of nearly symmetric divisions for the system $^{56}\text{Fe} + ^{238}\text{U}$, asymmetric fission of ^{238}U following deep-inelastic collisions could contribute to the observed yield, making it an upper limit. This corresponds to a lower limit for the additional energy ΔE. For the points taken from unpublished material, the solid circles[42] refer to the formation of ^{246}Fm through the reactions $^{40}\text{Ar} + ^{206}\text{Pb}$, $^{76}\text{Ge} + ^{170}\text{Er}$, $^{86}\text{Kr} + ^{160}\text{Gd}$, and $^{110}\text{Pd} + ^{136}\text{Xe}$, the solid triangles[41] refer to the reactions $^{50}\text{Ti} + ^{208}\text{Pb} \rightarrow ^{258}104$ and $^{50}\text{Ti} + ^{209}\text{Bi} \rightarrow ^{259}105$, and the open square[45] refers to the reaction $^{76}\text{Ge} + ^{170}\text{Er} \rightarrow ^{246}\text{Fm}$.

As seen in Fig. 12, all experimental values of ΔE taken together agree much better with the results calculated for two-body viscosity than with the results calculated for either type of one-body dissipation. Also, we note that if one were to correct the wall-and-window curve, allowing for the use of a smaller transition radius r_n, the resulting curve would be displaced to the left, thus enhancing the apparent disagreement with experiment. However, because the solid symbols usually lie somewhat above the open symbols, and because the error bars for the three solid symbols with the largest values of $(Z^2/A)_{\text{mean}}$ extend to $+\infty$, these conclusions must be regarded as tentative.

V. SUMMARY AND CONCLUSIONS

On the basis of a macroscopic dynamical model, we have calculated the dependence upon Z^2/A of the additional energy ΔE relative to the maximum in the one-dimensional interaction barrier required for compound-nucleus formation in symmetric heavy-ion reactions. This was done by solving numerically the classical equations of motion for head-on collisions within the three-quadratic-surface shape parametrization for zero dissipation, ordinary two-body viscosity, one-body wall-formula dissipation, and one-body wall-and-window dissipation.

Studying first the sensitivity of the calculated results to various details of the model, we found that for zero dissipation the YPE energy leads to a more compact saddle-point shape than does the SY energy, thus requiring a slightly larger ΔE. Similarly, we found that constraining the spheroidal ends of the system to be spherical increases the additional energy ΔE somewhat for zero dissipation, but decreases it for two-body viscosity and both types of one-body dissipation considered. Our most significant finding was that the calculated values of ΔE for both types of one-body dissipation are in general an order of magnitude larger than those for zero dissipation and ordinary two-body viscosity.

By use of a tentative scaling involving the geometric mean $(Z^2/A)_{\text{mean}}$, we compared our results calculated for symmetric systems with experimental values of ΔE for asymmetric systems. The experimental values agree much better with the results calculated for two-body viscosity than with the results calculated for either type of one-body dissipation. However, for the larger values of $(Z^2/A)_{\text{mean}}$, the current experimental values extracted from evaporation-residue measurements, which represent the only definitive proof of compound-nucleus formation, have error

bars that extend to $+\infty$.

In conclusion, we seem to be on the brink of determining the magnitude and mechanism of nuclear dissipation, but to do this unambiguously we need further evaporation-residue measurements for heavy nearly symmetric systems and/or calculations performed for asymmetric systems.

ACKNOWLEDGMENTS

We are grateful to H. Feldmeier, H. Gäggeler, F. Plasil, and W. J. Swiatecki for stimulating discussions. This research was supported by the U.S. Department of Energy under a contract with the University of California and Contract W-7405-eng-26 with the Union Carbide Corporation.

APPENDIX A: MODEL OF NECK FORMATION

A realistic model for the formation of a neck between two interacting nuclei near the point of first contact poses some serious difficulties. Because we are unable to accurately describe the dynamics of the nuclear fluid for the large distortions and rapid motions occurring when the neck is first forming in a heavy-ion collision, we use a simpler approximation near the contact point.

The interaction energy as a function of the separation between two spherical nuclei interacting via the long-range Coulomb repulsive force and the short-range nuclear attractive force initially increases as the nuclei are brought together, due to the dominance of the Coulomb repulsion at large distances. When they are sufficiently close that the short-range nuclear attractive force just balances the Coulomb force, a maximum in the one-dimensional interaction barrier occurs. For the model of the nuclear force that we use, the maximum in the barrier is situated outside the point where the equivalent sharp surfaces of the nuclei touch for systems with combined mass numbers less than about 300.

If we allow the two nuclei to deform in response to the forces between them as we bring them together, the Coulomb forces will tend to make them oblate. When they are close enough for the nuclear forces to act appreciably, these forces will tend to deform the nuclei so that they become prolate, eventually forming a neck between them as they get closer together. The time development of this process depends very sensitively on the details of the model used to describe it, so that it is not clear whether the nuclei would be oblate or prolate when they reach the point at which the neck forms. For example, the inertia with respect to deformation of a nucleus far away from another is nearly the same as for the isolated nucleus. However, when the nuclei are nearly in contact, the presence of the second nucleus changes the structure of the first, leading to a somewhat different inertia.

The location of a diffuse surface like that of a nucleus is an imprecise concept. For concreteness we define the nuclear surface as the surface on which the density of nuclear matter is one-half its average interior value and then consider the evolution of this surface as two nuclei are brought together.[19] First, consider the case where two spherical, frozen, diffuse matter distributions are brought together. Initially, the half-density surfaces of the nuclei are spherical. As their density tails begin to overlap appreciably, the surfaces bulge toward each other and eventually join the separated shapes into a single-necked shape. At this touching point, the radius of the neck grows infinitely fast for a finite velocity of approach of the two nuclei. However, other than the overall center-of-mass motion of the two nuclei, no matter has moved during the entire process just described. In addition to this geometrical neck formation, there is in general a dynamical evolution of the nuclear shape corresponding to motion of matter with respect to the centers of mass of the interacting nuclei. Therefore, the formation of the nuclear neck is a combination of a geometrical process with trivial dynamical content and a dynamical process involving the properties of nuclear matter.[19]

Because of the competing directions of the nuclear and Coulomb forces of deformation, and because we lack a convincing model for the inertias for deformations, we constrain the nuclei to remain spherical in their approach phase. This constraint is imposed until the radius of the neck reaches a specified value, which is usually taken to be 3.0 fm. At this point we begin the full dynamical evolution of the shape, using the equations given in the text. For the general case with angular momentum, we use an analytic Coulomb hyperbolic orbit to describe the approach of the two nuclei from infinite separation to the point where the Yukawa-plus-exponential nuclear interaction energy has the negligibly small value -0.01 MeV. From this point on, we integrate numerically the equation of motion for the separation r between the centers of mass of the nuclei. The potential energy is the sum of the Coulomb energy and the Yukawa-plus-exponential nuclear macroscopic energy, and the inertia with respect to r is calculated for point masses. We calculate the potential energy during the geometrical-neck-growth phase for a three-quadratic-surface shape whose hyperboloidal neck contains the matter from the region of overlap of the two spheres. Since we assume that no dynamical deformations occur during the approach phase, we use only the dissipative forces of Randrup's approximate proximity window dissipation model,[65] which takes into account the momentum transfer between the two nuclei when single particles pass through the window. At the starting point of the full dynamical evolution, we keep both r and dr/dt continuous.

Our choice of 3.0 fm for the transition neck radius was motivated partly for computational convenience and partly by the fact that fission-fragment kinetic energies for the fission of nuclei throughout the Periodic Table are optimally reproduced with wall-and-window dissipation when the transition from the pure wall formula is made at a neck radius of 3.0 fm.[58] Even with such a relatively large neck radius at the start of the full shape evolution, the fractional volume of matter removed from the overlap region of the two spherical nuclei is only 0.5% for the ^{220}U system.

A transition neck radius of 3.5 fm was used for the wall-and-window calculations because this type of dissipation greatly restricts the growth of the neck, which leads to the formation of a cusp between the end bodies when the 3.0-fm starting neck radius is used. As seen in Table I, when the end bodies are constrained to be spherical, increasing the transition neck radius from 3.0 to 3.5 fm decreases the calculated additional energy ΔE from 36 to 32

MeV. Also, for zero dissipation in the full three-quadratic-surface parametrization, increasing the transition neck radius from 1.0 to 3.0 fm decreases ΔE from 3.8 to 0 MeV.

APPENDIX B: FUNCTIONAL DEPENDENCE OF ΔE ON $Z^2/A-(Z^2/A)_{\rm thr}$

We now consider the behavior of the fusing system near the threshold for compound-nucleus formation, and the effects the details of the model have on the results. For a system of critical size, which will just form a compound nucleus if the nuclei reach the top of the interaction barrier with no remaining kinetic energy, the potential energy has three relevant characteristics:

(1) The fission saddle point lies at (r_0,σ_0) and the maximum in the interaction barrier at (r_b,σ_b), with $r_0\approx r_b$ and $\sigma_0>\sigma_b$.

(2) The energy at the barrier top is greater than the saddle-point energy.

(3) The force on the system at the top of the interaction barrier is in the general direction of the saddle point.

If we neglect dissipative forces and deformations occurring before reaching the top of the interaction barrier, at the threshold for compound-nucleus formation the critically sized systems with $Z^2/A=(Z^2/A)_{\rm thr}$ will start from rest at (r_b,σ_b) and subsequently follow a trajectory that passes through (r_0,σ_0) in time T_0. A slightly heavier system with

$$Z^2/A=(Z^2/A)_{\rm thr}+\Delta(Z^2/A)$$

has its saddle point located at $(r_0-\Delta r_0,\sigma_0-\Delta\sigma_0)$, where $\Delta r_0=\alpha\Delta(Z^2/A)$ and $\Delta\sigma_0=\beta\Delta(Z^2/A)$ to first order in $\Delta(Z^2/A)$, with α and β positive constants. This system, if started from rest at the top of the new barrier located very close to (r_b,σ_b), would follow a trajectory nearly the same as the previous one, passing outside the new saddle point and consequently reseparating. In order to just pass through the saddle point, the system must be given an initial component of velocity in the $-r$ direction. In the simplest case, where the velocity at the barrier is purely in the r direction, the forces in the r direction are negligible, $\Delta\sigma_0\ll\sigma_0-\sigma_b$, and the inertia is nearly diagonal with respect to the r and σ directions, the system travels the additional distance Δr_0 inward during the time T_0 when the initial radial velocity at the barrier top is

$$v_r=-\Delta r_0/T_0=\frac{-\alpha}{T_0}\Delta(Z^2/A)\ .$$

In terms of the additional energy that is required, we may express this relationship to lowest order as

$$\Delta E=\gamma[\Delta(Z^2/A)]^2\ ,$$

a result found empirically by Swiatecki.[20–22]

In our model, because we prevent the nuclei from deforming in the σ direction until they are well inside the interaction barrier, they have (in the absence of infinite dissipative forces) a finite v_r at their starting point, even though they reached the top of the barrier with zero kinetic energy. For example, for the ^{220}U system the energy of the tangent-sphere configuration is 1 MeV below that of the barrier top, and the energy of the shape with a 3.0-fm neck radius is 6 MeV below that of the barrier top. In this case, the slightly different critically sized system starts off at the point (r_s,σ_s), where $r_s<r_b$ and $\sigma_s\approx\sigma_b$, with a velocity v_1 directed radially inward and kinetic energy $E_1=\frac{1}{2}M_r v_1^2$, where M_r is the inertia for motion in the r direction. It reaches the saddle point (r_1,σ_1) in a time T_1, which is again mainly determined by the forces acting in the σ direction. A slightly heavier system with its saddle point at $(r_1-\Delta r_1,\sigma_1-\Delta\sigma_1)$ needs an initial velocity of $v_1+\Delta v_1$, where $\Delta v_1=-\Delta r_1/T_1$, to reach the saddle point. Again neglecting dissipation, we find that the additional kinetic energy required at the barrier top is

$$\Delta E=\tfrac{1}{2}M_r(v_1+\Delta v_1)^2-E_1=M_r\Delta v_1(v_1+\tfrac{1}{2}\Delta v_1)\ ,$$

or

$$\Delta E=\delta[\Delta(Z^2/A)]+\gamma'[\Delta(Z^2/A)]^2\ .$$

Therefore, constraining the nuclei to remain spherical until inside the barrier top adds a linear term in the dependence of ΔE on $\Delta(Z^2/A)$. Whereas this constraint may be appropriate at energies well above the top of the barrier, it should be less appropriate for energies near the barrier top because of the deformations that are expected to occur during the relatively long time the system spends moving slowly there.

To conclude, since the functional dependence of ΔE on $\Delta(Z^2/A)$ near threshold depends sensitively on the details of the model used to describe the approach and initial contact stages, the important quantity to consider is not $(Z^2/A)_{\rm thr}$, but instead the shape of the function in the region where ΔE is experimentally distinguishable from zero.

[1] W. J. Swiatecki, in *Proceedings of the International Conference on Nuclear Reactions Induced by Heavy Ions, Heidelberg, Germany, 1969,* edited by R. Bock and W. R. Hering (North-Holland, Amsterdam/American Elsevier, New York, 1970), p. 729.

[2] W. J. Swiatecki, J. Phys. Suppl. 33, C5–45 (2972).

[3] W. J. Swiatecki and S. Bjørnholm, Phys. Rep. 4C, 325 (1972).

[4] J. R. Nix, in Proceedings of the International Conference on the Properties of Nuclei Far from the Region of Beta-Stability, Leysin, Switzerland, 1970, CERN Report No. CERN-70-30, 1970 (unpublished), Vol. 2, p. 605.

[5] J. R. Nix, Phys. Today 25, No. 4, 30 (1972).

[6] J. R. Nix, in Proceedings of the 5th Summer School on Nuclear Physics, Rudziska, Poland, 1972, edited by E. Cieslak, M. Dabrowska, and A. Saganek, Institute of Nuclear Research Report No. INR-P-1447/I/PL, 1972 (unpublished), Vol. 1, p. 299.

[7] J. R. Nix, Annu. Rev. Nucl. Sci. 22, 65 (1972).

[8] A. J. Sierk and J. R. Nix, in *Proceedings of the Third International Atomic Energy Agency Symposium on the Physics and Chemistry of Fission, Rochester, New York, 1973* (IAEA, Vienna, 1974), Vol. II, p. 273.

[9] J. R. Nix and A. J. Sierk, Phys. Scr. 10A, 94 (1974).

[10] J. R. Nix and A. J. Sierk, in Proceedings of the XIII International Winter Meeting on Nuclear Physics, Bormio, Italy, 1975, University of Milan report, 1975 (unpublished), p. 1.

[11]J. R. Nix and A. J. Sierk, in Proceedings of the International School—Seminar on Reactions of Heavy Ions with Nuclei and Synthesis of New Elements, Dubna, USSR, 1975, Joint Institute for Nuclear Research Report No. JINR-D7-9734, 1976 (unpublished), p. 101.
[12]A. J. Sierk and J. R. Nix, in Proceedings of the Symposium on Macroscopic Features of Heavy-Ion Collisions, Argonne, Illinois, 1976, Argonne National Laboratory Report No. ANL-PHY-76-2, 1976 (unpublished), Vol. I, p. 407.
[13]J. R. Nix and A. J. Sierk, Phys. Rev. C 15, 2072 (1977).
[14]A. J. Sierk and J. R. Nix, Phys. Rev. C 16, 1048 (1977).
[15]A. A. Amsden, A. S. Goldhaber, F. H. Harlow, P. Möller, J. R. Nix, and A. J. Sierk, in Proceedings of the IPCR Symposium on Macroscopic Features of Heavy-Ion Collisions and Pre-equilibrium Process, Hakone, Japan, 1977, IPCR Cyclotron Progress Report, Supplement 6, 1977 (unpublished), p. 235.
[16]A. J. Sierk, in *Proceedings of the International Symposium on Superheavy Elements, Lubbock, Texas, 1978,* edited by M. A. K. Lodhi (Pergamon, New York, 1978), p. 479.
[17]J. R. Nix, S. Afr. J. Phys. 1, 103 (1978).
[18]J. R. Nix, in *Proceedings of the International Conference on Nuclear Interactions, Canberra, Australia, 1978,* edited by B. A. Robson (Springer, Berlin, 1978), p. 140.
[19]W. J. Swiatecki, Prog. Part. Nucl. Phys. 4, 383 (1980).
[20]W. J. Swiatecki, Phys. Scr. 24, 113 (1981).
[21]W. J. Swiatecki, in Proceedings of the 4th International Conference on Nuclei Far from Stability, Helsingør, Denmark, 1981, CERN Report No. CERN-81-09, 1981 (unpublished), p. 781.
[22]W. J. Swiatecki, Nucl. Phys. A376, 275 (1982).
[23]S. Bjørnholm and W. J. Swiatecki, Nucl. Phys. A391, 471 (1982).
[24]J. Błocki and W. J. Swiatecki (unpublished).
[25]H. Feldmeier, in Proceedings of the International Workshop X on Gross Properties of Nuclei and Nuclear Excitations, Hirschegg, Austria, 1982, edited by H. Feldmeier, Technische Hochschule Darmstadt Report ISSN-0720-8715, 1982, p. 26.
[26]J. Błocki and M. Dworzecka, Bull. Am. Phys. Soc. 27, 550 (1982).
[27]K. T. R. Davies and S. E. Koonin, Phys. Rev. C 23, 2042 (1981). Comprehensive lists of TDHF references are found in this paper and in the review articles, Refs. 28 and 29.
[28]K. T. R. Davies, K. R. S. Devi, S. E. Koonin, and M. R. Strayer, in *Heavy Ion Science, Nuclear Science,* edited by D. A. Bromley (Plenum, New York, to be published), Vols. I and II.
[29]J. W. Negele, Rev. Mod. Phys. 54, 913 (1982).
[30]P. Bonche, K. T. R. Davies, B. Flanders, H. Flocard, B. Grammaticos, S. E. Koonin, S. J. Krieger, and M. S. Weiss, Phys. Rev. C 20, 641 (1979).
[31]K. T. R. Davies, K. R. S. Devi, and M. R. Strayer, Phys. Rev. Lett. 44, 23 (1980).
[32]K. T. R. Davies, K. R. S. Devi, and M. R. Strayer, Phys. Rev. C 24, 2576 (1981).
[33]H. Stöcker, R. Y. Cusson, H. J. Lustig, A. Gobbi, J. Hahn, J. A. Maruhn, and W. Greiner, Z. Phys. A 306, 235 (1982).
[34]H. Sann, R. Bock, Y. T. Chu, A. Gobbi, A. Olmi, U. Lynen, W. Müller, S. Bjørnholm, and H. Esbensen, Phys. Rev. Lett. 47, 1248 (1981).
[35]R. Bock, Y. T. Chu, M. Dakowski, A. Gobbi, E. Grosse, A. Olmi, H. Sann, D. Schwalm, U. Lynen, W. Müller, S. Bjørnholm, H. Esbensen, W. Wölfli, and E. Morenzoni, Nucl. Phys. A388, 334 (1982).
[36]S. Bjørnholm, in Proceedings of the International Workshop X on Gross Properties of Nuclei and Nuclear Excitations, Hirschegg, Austria, 1982, edited by H. Feldmeier, Technische Hochschule Darmstadt Report ISSN-0720-8715, 1982, p. 15.
[37]S. Bjørnholm in *Proceedings of the Nuclear Physics Workshop, Trieste, Italy, 1981,* edited by C. H. Dasso, R. A. Broglia, and A. Winther (North-Holland, Amsterdam, 1982), p. 521.
[38]S. Bjørnholm, Nucl. Phys. A387, 51c (1982).
[39]S. Bjørnholm, Comments Nucl. Part. Phys. 11, 9 (1982).
[40]J. R. Huizenga, J. R. Birkelund, W. U. Schröder, W. W. Wilcke, and J. J. Wollerscheim, in *Proceedings of the 3rd Adriatic Europhysics Study Conference on the Dynamics of Heavy-Ion Collisions, Hvar, Yugoslavia, 1981,* edited by N. Cindro, R. A. Ricci, and W. Greiner (North-Holland, Amsterdam, 1981), p. 15.
[41]H. Gäggeler, W. Brüchle, J. V. Kratz, M. Schädel, K. Sümmerer, G. Wirth, and T. Sikkeland, in Proceedings of the International Workshop X on Gross Properties of Nuclei and Nuclear Excitations, Hirschegg, Austria, 1982, edited by H. Feldmeier, Technische Hochschule Darmstadt Report ISSN-0720-8715, 1982, p. 40.
[42]H. Gäggeler (unpublished).
[43]W. Westmeier, R. A. Esterlund, A. Rox, and P. Patzelt, Phys. Lett. 117B, 163 (1982).
[44]B. Sikora, J. Bisplinghoff, M. Blann, W. Scobel, M. Beckerman, F. Plasil, R. L. Ferguson, J. Birkelund, and W. Wilcke, Phys. Rev. C 25, 686 (1982).
[45]K. Luetzenkirchen, University of Mainz diploma work, 1982 (unpublished).
[46]D. H. E. Gross and L. Satpathy, Phys. Lett. 110B, 31 (1982).
[47]K. H. Schmidt, P. Armbruster, F. P. Hessberger, G. Münzenberg, W. Reisdorf, C. C. Sahm, D. Vermeulen, H. G. Clerc, J. Keller, and H. Schulte, Z. Phys. A 301, 21 (1981).
[48]J. R. Nix, Nucl. Phys. A130, 241 (1969).
[49]K. T. R. Davies, A. J. Sierk, and J. R. Nix, Phys. Rev. C 13, 2385 (1976).
[50]A. J. Sierk and J. R. Nix, Phys. Rev. C 21, 982 (1980).
[51]P. Möller and J. R. Nix, Nucl. Phys. A272, 502 (1976).
[52]H. J. Krappe, J. R. Nix, and A. J. Sierk, Phys. Rev. Lett. 42, 215 (1979).
[53]H. J. Krappe, J. R. Nix, and A. J. Sierk, Phys. Rev. C 20, 992 (1979).
[54]P. Möller and J. R. Nix, Nucl. Phys. A361, 117 (1981).
[55]P. Möller and J. R. Nix, At. Data Nucl. Data Tables 26, 165 (1981).
[56]H. J. Krappe and J. R. Nix, in *Proceedings of the Third International Atomic Energy Agency Symposium on the Physics and Chemistry of Fission, Rochester, New York, 1973* (IAEA, Vienna, 1974), Vol. I, p. 159.
[57]W. D. Myers and W. J. Swiatecki, Ark. Fys. 36, 343 (1967).
[58]A. J. Sierk (unpublished).
[59]J. Błocki, Y. Boneh, J. R. Nix, J. Randrup, M. Robel, A. J. Sierk, and W. J. Swiatecki, Ann. Phys. (N.Y.) 113, 330 (1978).
[60]J. Randrup and W. J. Swiatecki, Ann. Phys. (N.Y.) 125, 193 (1980).
[61]H. Goldstein, *Classical Mechanics* (Addison-Wesley, Reading, Mass., 1959), Chap. 1, Sec. 5, pp. 19—22.
[62]C. Ngô, C. Grégoire, and B. Remaud, in *Proceedings of the 3rd Adriatic Europhysics Study Conference on the Dynamics of Heavy-Ion Collisions, Hvar, Yugoslavia, 1981,* edited by N. Cindro, R. A. Ricci, and W. Greiner (North-Holland, Amsterdam, 1981), p. 211.
[63]A. E. S. Green, *Nuclear Physics* (McGraw-Hill, New York, 1955), pp. 185, 250.
[64]J. Błocki, J. Randrup, W. J. Swiatecki, and C. F. Tsang, Ann. Phys. (N.Y.) 105, 427 (1977).
[65]J. Randrup, Ann. Phys. (N.Y.) 112, 356 (1978).